

Observation of internal pulsed current flow through the ZnO specimen in the spark plasma sintering method

Tatsuya Misawa · Noboru Shikatani · Yuji Kawakami · Takashi Enjoji · Yasunori Ohtsu · Hiroharu Fujita

Received: 1 February 2008 / Accepted: 24 July 2008 / Published online: 10 September 2008
© Springer Science+Business Media, LLC 2008

Abstract In spark plasma sintering (SPS), it is supposed that a part of the large pulsed sintering current flows into the specimen and affects the sintering behavior. To clarify the influence of the internal pulsed current that flows through the specimen during SPS, measurement of the electrical resistance of the specimen was conducted using Pt electrodes and the internal pulsed current was successfully observed using a magnetic probe during the sintering of ZnO and other materials. Two Pt electrodes were installed on the sides of a ZnO sample through a carbon die, and decrease of electrical resistance was observed with the progress of sintering. The internal current that flows through the specimen during SPS was several hundred ampere, and the ratio of the internal current to the total current was found to be dependent on the material and the progress of SPS process.

Introduction

Spark plasma sintering (SPS) or pulsed current sintering (PCS) methods, which enable high-quality and wide material-selectivity sintering within a comparatively small time, have been investigated in recent years [1–8]. In particular, it has been supposed that during the SPS process, a part of the large pulsed sintering current (several kA) flows into the specimen and affects the sintering behavior; therefore, the role of internal current on the SPS process is very important in order to understand the sintering behavior.

Numerical study of the current and temperature distribution in conductive and non-conductive materials and sintering containers has been carried out using the finite volume method, and the theoretical and experimental results were compared [6]. In addition, a fundamental investigation and discussion regarding field activated sintering processes, including the effect of internal current on PCS or SPS processes, has been deduced from various experimental and theoretical research [8].

The research suggests that the amount, spatial distribution, and temporal behavior of internal current in the sintering body are determined by progress of sintering and the electrical properties of the materials being sintered during the process, and simultaneously, the behavior of the internal current self-consistently affects the progress of the sintering. Therefore, in situ, simultaneous and quantitative measurements of the internal current flow through a sintering specimen are very important in order to understand the SPS process; however, only a few experiments which directly measure the internal current have been carried out to date.

In order to develop a quantitative method for the measurement of internal current and clarification of the sintering behavior during the SPS process, direct measurement of

T. Misawa (✉) · Y. Ohtsu · H. Fujita
Department of Electrical and Electronic Engineering,
Faculty of Science and Engineering, Saga University,
1 Honjyo-machi, Saga 840-8502, Japan
e-mail: misawa@ep.ee.saga-u.ac.jp

N. Shikatani
Department of Life, Environment and Material Science,
Faculty of Engineering, Fukuoka Institute of Technology,
3-30-1 Wajiro-higashi, Higashiku,
Fukuoka 811-0295, Japan

Y. Kawakami · T. Enjoji
Department of Material and Environment, Industrial Technology
Center of Saga, 114 Yaemizo, Nabeshima-machi,
Saga 849-0932, Japan

electrical resistance using Pt electrodes and magnetic non-touching measurements were conducted for quantitative estimation of the internal current. This investigation aims to propose a new evaluation method that can non-destructively and quantitatively indicate the dynamic behavior of spark plasma sintering during the SPS process.

Experimental setup

Detail of experimental device

The experiment was carried out in a spark plasma sintering device (SPS-3.20 MK-IV, SPS Syntex Inc., Kanagawa, Japan). The powdered material was enclosed in a carbon graphite die and punch, compressed by hydraulic press mechanism, and heated by application of a pulsed sintering current under low gas pressure (Fig. 1). The cylindrical sintering die has a 30 mm inner diameter, 70 mm outer diameter, and 60 mm height. Holes were opened on the side of sintering die for insertion of the electrodes, thermocouple, and magnetic probe. Typical experimental parameters used were: sintering voltage $V_s = 5$ V, sintering current $I_s = 3$ kA, temperature $T = 1273$ K, compressing force $P_{\text{compress}} = 30$ MPa, gas pressure $P_{\text{gas}} = 5$ Pa.

In this experiment, Cu powder and ZnO powder with small additions of Al_2O_3 , TiO_2 , and CoO were used. Cu powder was produced by Katayama Chemical Ltd., Osaka, Japan, and mean diameter and purity of Cu powder is 75 μm and 99.5%, respectively. The electric resistance of the ZnO specimen with a small amount of Al_2O_3 decreases the progress of sintering. Therefore, it was considered that the

internal current which passes through the specimen changes the progress of the SPS process. ZnO, Al_2O_3 , TiO_2 , and CoO raw powder were produced by Kojundo Chemical Lab. Co., Ltd., Saitama, Japan. The particle diameters of the ZnO, Al_2O_3 , TiO_2 , and CoO powder materials were approximately 1–2 μm , and the purity are 99.9% of ZnO, Al_2O_3 , TiO_2 , and 99.0% of CoO, respectively. The raw materials were ball milled in methanol for 24 h, and dried under vacuum for 12 h. The compositional molar ratio of the mixed powder was $\text{ZnO}:\text{Al}_2\text{O}_3:\text{TiO}_2:\text{CoO} = 100:2:2:2$.

Measurement of electrical resistance

For simultaneous measurement of the electrical resistance of the sintering material during SPS processing, two Pt electrodes and Pt thermocouple were installed inside the ZnO powder material through the carbon graphite sintering die, as shown in Fig. 2a. The distance between the Pt electrodes (0.5 mm \varnothing) was 20 mm, and the length of exposure in the specimen was 2 mm. A Pt thermocouple was located in the center of the specimen.

Pt electrodes were connected to a measurement circuit composed of a constant-current power supply and resistance (Fig. 2b). The voltage between the edge of the Pt electrodes was measured, and the current was evaluated from the voltage in the resistance circuit. The resistance of the sintering specimen was then estimated from the voltage and current between the Pt electrodes. Internal temperature, voltage, and current were recorded by a data logger during the sintering process. Generally, pulsed high power equipment such as SPS devices often have large electrical and magnetic noise and fluctuations in the standard potential of the device, despite accurately taking into account the earth potential of the device.

Magnetic measurement of internal pulsed current flow in the sintering specimen

During the SPS process, a pulsed sintering current of several kA passes into the sintering mold, and a part of the sintering current flows into the specimen. Therefore, internal current can generate a pulsed magnetic field around the specimen and sintering mold. Because the sintering current temporally changes, theoretically, the magnetic field can be easily detected using a simple magnetic probe composed of a single turn or several turn coil. Therefore, if it is assumed that the current distribution is axially symmetric in the sintering mold and specimen, the amount of internal current that flows in the specimen can be evaluated from the magnetic field measured by a magnetic probe located at the side of the sintering specimen.

Schematics of the magnetic probe measurement are shown in Fig. 3. The magnetic probe is a Ni coil with a

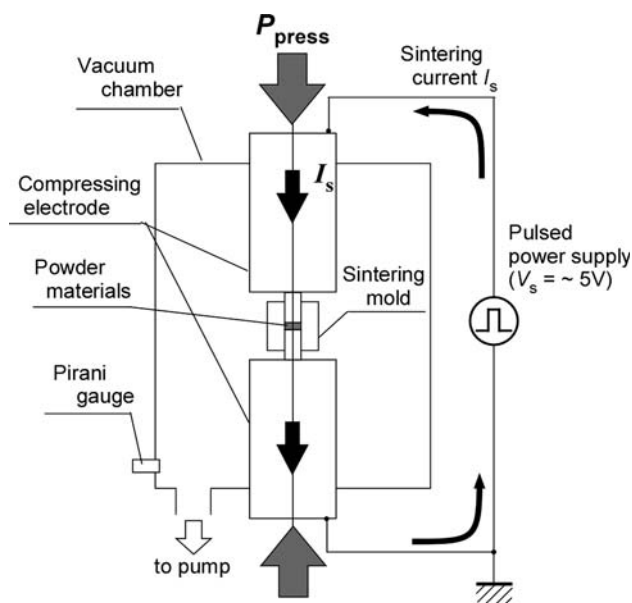


Fig. 1 Schematics of SPS device

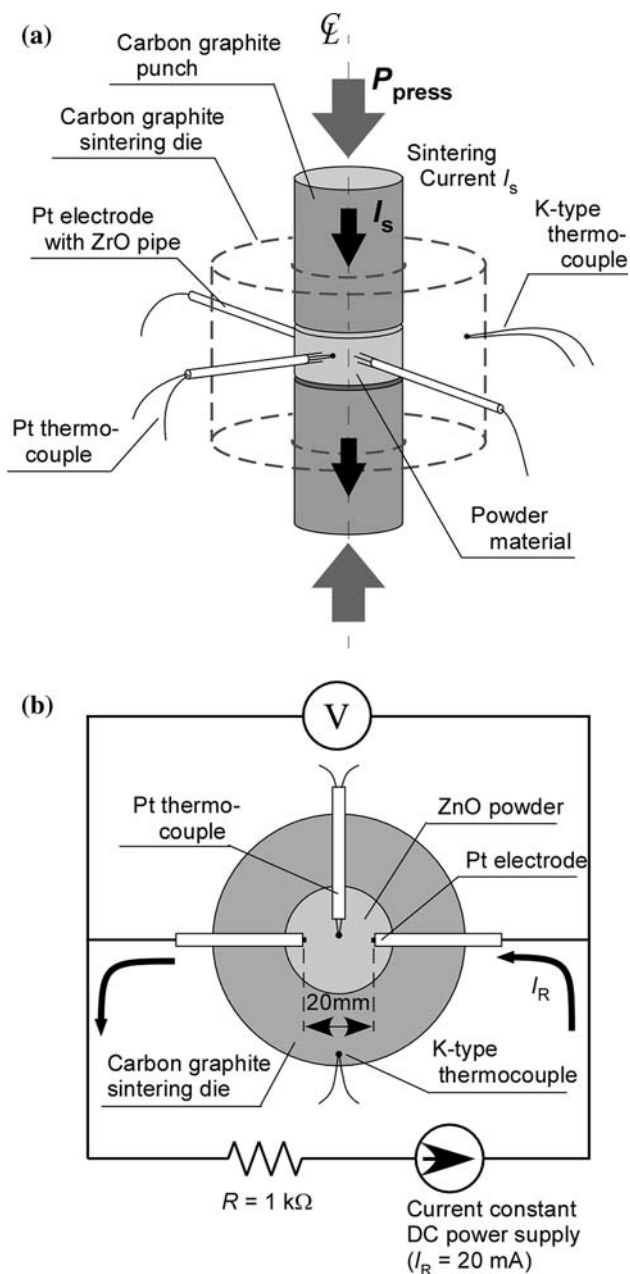


Fig. 2 Sintering mold and measurement circuit. (a) Sintering mold and Pt electrode and (b) measurement system of temperature and electric resistance of ZnO specimen

coaxial structure composed of Ni wire, Ni tube, and Al_2O_3 tubes. The magnetic probe is exposed to high temperatures of 1500 K; therefore, it is necessary that all materials of the magnetic probe have sufficient heat resistance. The inner diameter of the coil is 3 mm, the winding number of coil is four turns, and the surface of the coil is coated with a zirconia adhesive.

The SPS device generates strong magnetic noise around the sintering mold and device during sintering, and the signal from magnetic probe is weak and may be masked by

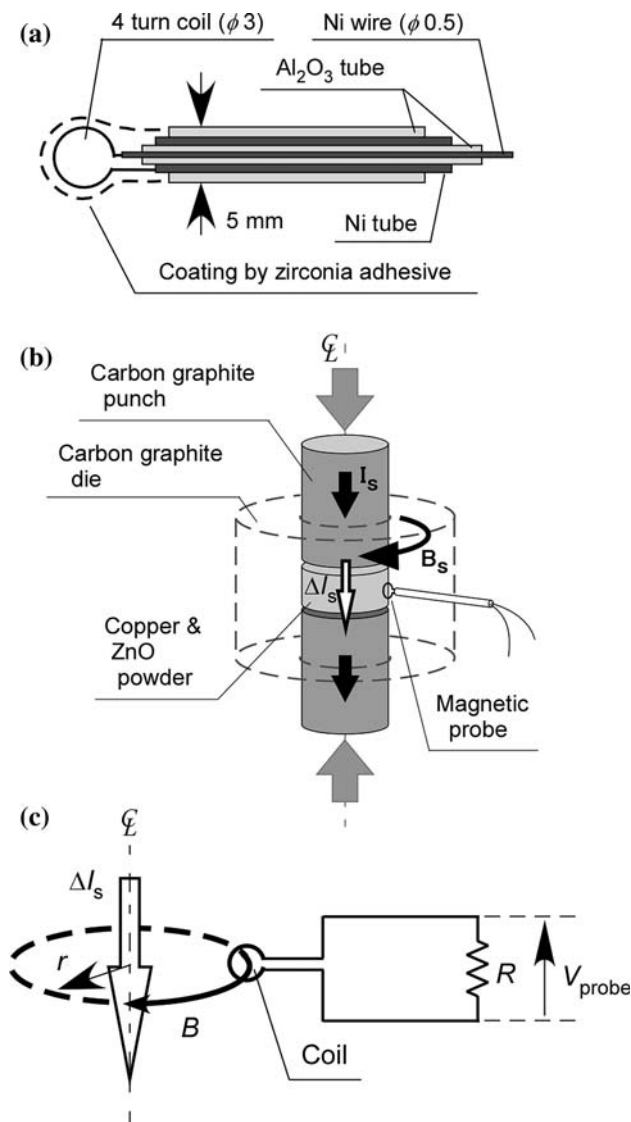


Fig. 3 Schematics of magnetic probe measurement system. (a) Cross section of coaxial magnetic probe, (b) relative position of magnetic probe and sintering specimen, and (c) measurement circuit

this noise. The coaxial structure of the probe and cable was used in order to decrease the influence of magnetic noise as much as possible.

The magnetic probe was installed to the side of the sintering specimen, so that the magnetic field is associated at right-angles to the coil in order to obtain the maximum signal (Fig. 3b, c). However, the signal from the magnetic probe under typical experimental conditions was evaluated as several μV . In addition, the signal obtained from magnetic probe also contains low frequency thermo-electromotive force with the high frequency magnetic signal of approximately 360 Hz. Therefore, a high gain amplifier was used to remove the low frequency signal and amplify the weak signal of the magnetic probe. The gain of the amplifier is 13,000 times, and signals of 70 Hz or less are sufficiently

attenuated. For reduction of magnetic noise, the amplifier was installed in a soft iron magnetic shielding box. And the shielding box and the digital oscilloscope were placed in the position which left over 2 m from the SPS device.

The temperature of the sintering die, the signal of magnetic probe, and the raw signal of total current (i.e., non-averaged sintering current) were synchronously recorded by a digital oscilloscope.

The relationship between the current density \mathbf{i} and the magnetic flux density \mathbf{B} is defined by Ampere's law [9] (Rationalized MKSA expression):

$$\text{rot}\mathbf{B} = \mu_0 \mathbf{i} + \mu_0 \varepsilon_0 \frac{\partial \mathbf{E}}{\partial t}, \quad (1)$$

where μ_0 is magnetic permeability of vacuum, ε_0 is permittivity of vacuum, t is time, and \mathbf{E} is electric field. Exactly, the permeability of materials and graphite die should be applied instead of μ_0 in Eq. 1. However, the difference of permeability between materials, graphite and vacuum is negligibly small, and permeability of vacuum is applied in Eq. 1. The second term of the right side expression can be ignored in this case.

If it is assumed that the current distribution in the sintering mold is symmetrical, with respect to the axis of the sintering mold, the amplitude of the magnetic flux density that the sintering current generates can be expressed by

$$B = \frac{\mu_0}{2\pi r} \int_0^r i \, dr = \frac{\mu_0}{2\pi r} \Delta I_s, \quad (2)$$

where B is the amplitude of magnetic flux density, r is the radial position of the magnetic probe, i is the current density, and ΔI_s is the current that flows within the radius r of the probe position. The direction of the magnetic field agrees with the direction of the circumference vector.

Theoretically, if the center of the magnetic probe coil is located within the radius of the cylindrical specimen, ΔI_s represents the amount of current flow through the sintering specimen. Experimentally, it is difficult to locate the center of the coil exactly to the side surface of the sintering specimen, so that the current measured by the magnetic probe includes unnecessary signals that are derived from the position tolerance of the magnetic probe.

The relationship between the counter electromotive force v_{probe} measured by the magnetic probe and the magnetic flux density B , and the internal current ΔI_s would be expressed as:

$$\begin{aligned} v_{\text{probe}} &= -\frac{d\phi}{dt} = -\frac{d(NSB)}{dt}, \\ &= -\frac{NS\mu_0}{2\pi r} \frac{d\Delta I_s}{dt} \end{aligned} \quad (3)$$

where ϕ is the magnetic flux that crosses the multiple winding coil, N is the number of windings of the coil, and S

is the area of the coil. As this equation shows, the counter electromotive force obtained from the magnetic probe is proportional to the time derivative of the internal current. It is possible to evaluate the internal current by integrating the signal of the counter electromotive force from the magnetic probe with respect to time. The internal current is estimated as:

$$\Delta I_s = -\frac{2\pi r}{NS\mu_0} \int v_{\text{probe}} dt. \quad (4)$$

In this study, the internal current was evaluated by numerical integration of the signal from the magnetic probe recorded by a digital oscilloscope.

Experimental result

Measurement of electric resistance of specimen

Figure 4a shows the time evolution of internal temperature in the specimen and the surface temperature of the sintering die. The experimental sintering conditions were as follows; gas pressure in the device $P_{\text{gas}} = 5$ Pa, compressive pressure $P_{\text{press}} = 30$ MPa, heating rate $v_{\text{heat}} = 1$ K/s, maximum temperature $T_{\text{max}} = 1373$ K; the compressive pressure was applied throughout the sintering term and cooling term, and the sintering die was maintained at the maximum temperature for 10 min. The temperature difference between the specimen and the sintering die is shown in Fig. 4a. During the time of maximum temperature, the difference in temperature was approximately 200 K. It was found that the electrical resistance of the ZnO specimen drastically changes during the SPS process with the increase in the specimen temperature, as shown in Fig. 4b.

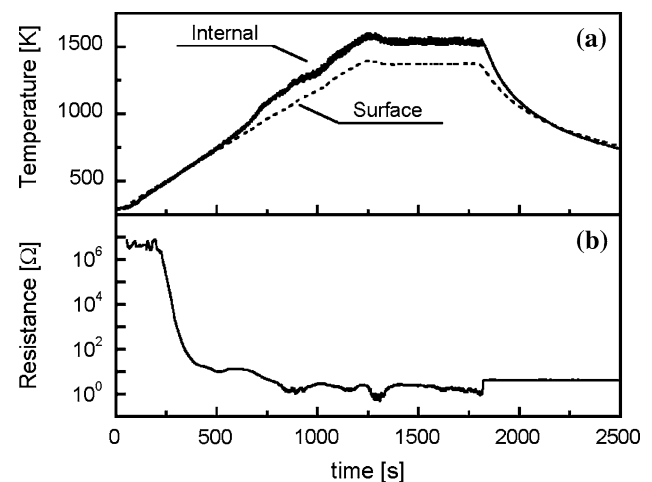


Fig. 4 Time evolution of temperature and electric resistance on ZnO sintering. (a) Temperature of specimen and sintering die and (b) electric resistance

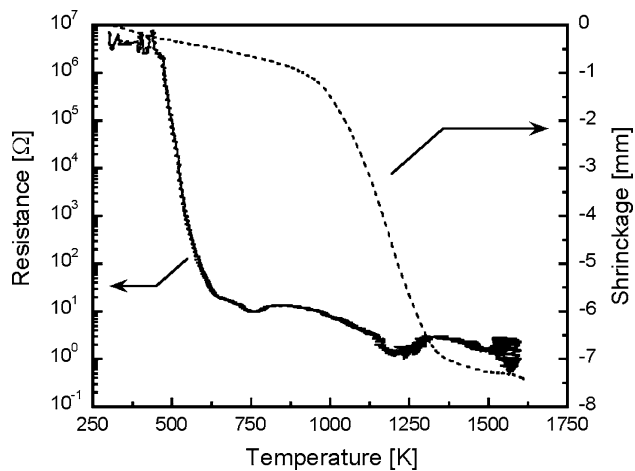


Fig. 5 Temperature dependence of electric resistance of ZnO specimen

Figure 5 shows the dependence of resistance on the internal temperature of the specimen. There are four temperature regions in which the change of resistance is different. The powder material is insulating in temperature region A, from room temperature to 450 K. The temperature of specimen is comparatively low; therefore, it is considered that sintering is not yet in progress. In temperature region B, between 450 and 600 K, the resistance of the powder material decreases significantly. The change in resistance reaches approximately 10^{-6} Ω , and the diminution rate is also very large at approximately 4 k Ω /s. It is anticipated that this drastic reduction of electric resistance is caused by oxygen vacancy in the ZnO materials, but exact reason was not clarified from present result. In temperature region C, between 600 and 1250 K, the resistance slowly decreases with the increase in temperature and becomes several ohm. Since the thickness of the sintering specimen is considerably decreased in the same temperature region, it is considered that the sintering of ZnO powder occurs mainly in this same temperature region, between 600 and 1250 K. In temperature region D, over 1250 K, the resistance becomes stable at approximately several ohm. The change in electrical resistance during SPS and the concomitant possible current flow through the sample can strongly influence the densification and microstructure of the material.

In order to compare the SPS process in a vacuum with the conventional sintering process and the SPS process under atmospheric pressure, sintering using same ZnO materials and graphite die was carried out using an atmospheric furnace under non-compression conditions, and the resulting resistance measurements are shown in Fig. 6. In the case of using an atmospheric furnace, the temperature at which the electrical resistance of the ZnO specimen decreases increased to 650 K during sintering, and the diminution rate of resistance was slow in comparison to that with the SPS process under vacuum conditions. In

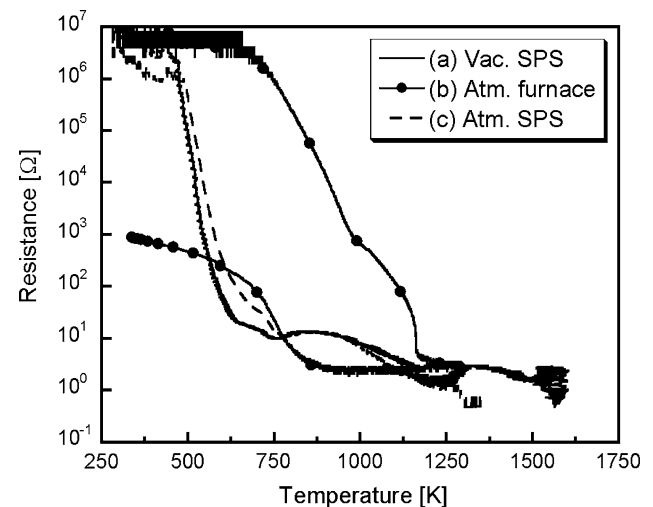


Fig. 6 Comparison of electric resistance under vacuum and atmospheric condition for SPS process and atmospheric furnace

addition, during the specimen cooling stage of, the resistance increased again from several ohm to 1000 Ω . On the other hand, in the case of using SPS in an air atmosphere, the temperature dependence of resistance was almost the same as that using SPS under vacuum conditions. These results indicate that a significant decrease of resistance occurs in the ZnO specimen during the SPS process, regardless of whether the process is performed under vacuum or air atmosphere conditions, and the internal current that flows in the ZnO specimen has a significant effect on the SPS process.

To observe the effect of internal current on the SPS process, a sintering experiment was carried out with internal current restriction using Al_2O_3 plates. In order to limit the internal current flow through the specimen, two Al_2O_3 plates (5 mm thickness and 30 mm diameter) were inserted into the boundary between the sintering punch and the powder material, and the sample was held from top and bottom, as shown in Fig. 7a. The results are shown in Fig. 7, using the same experimental conditions used as that for Figs. 4 and 5.

The temperature dependence of resistance for the ZnO specimen under the internal current limiting condition was almost the same as that under conventional conditions, as shown in Fig. 7b. However, a clear difference between the internal structure of the sintered specimen using the internal current limited condition and that under conventional conditions was observed. Figure 8 shows typical cross-sectional scanning electron microscope (SEM) images of the center point of ZnO specimen sintered with and without the internal current limitation. For the current limiting condition, the boundary of sintered particles is confirmed, and the particles seem to grow to a size of several micrometer, as shown in Fig. 8a. On the other hand, under

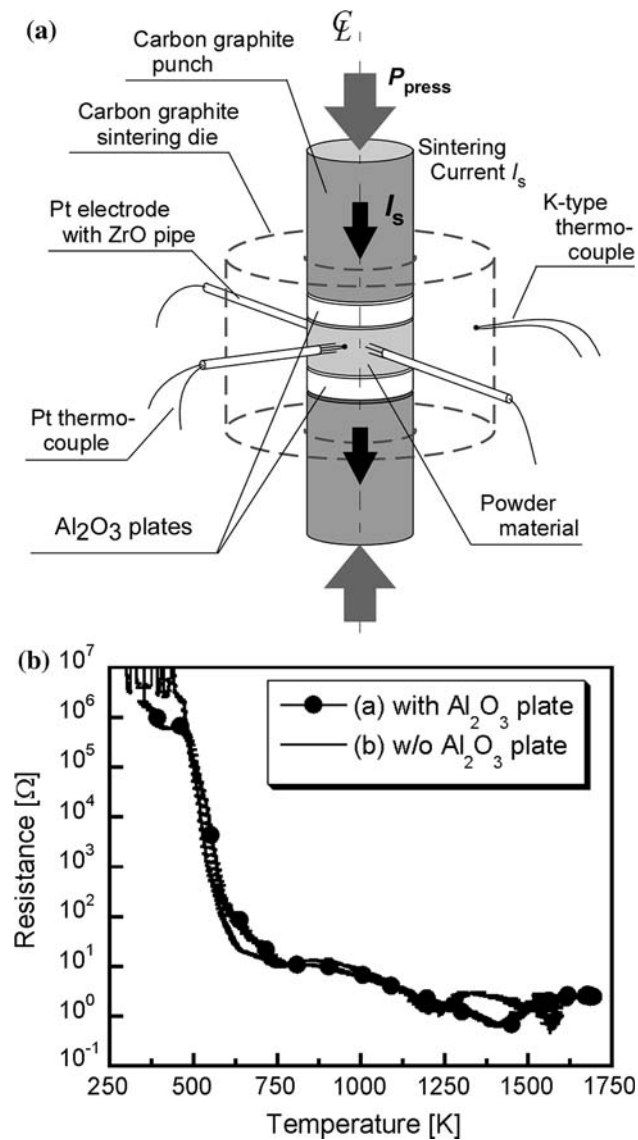


Fig. 7 SPS process under current limiting condition. (a) Schematics of sintering die with Al₂O₃ plates and (b) resistance with and without Al₂O₃ plates

conventional conditions, interparticle necking occurs, and it is not possible to clearly observe particle boundaries, as shown in Fig. 8b.

These results indicate that the internal current that flows through the sintering material during the SPS process affects the formation of the internal structure. (Please note that the electrical resistance for the sample using SPS with Al₂O₃ plates (*solid line* (a) in Fig. 7b) is rather similar to that using SPS in an air atmosphere (*broken line* (c) in Fig. 6), although these results are from different conditions.) The resistance reduction of ZnO specimen is more strongly affected by temperature condition rather than internal current, and temperature and resistance characteristics of current limited condition and conventional

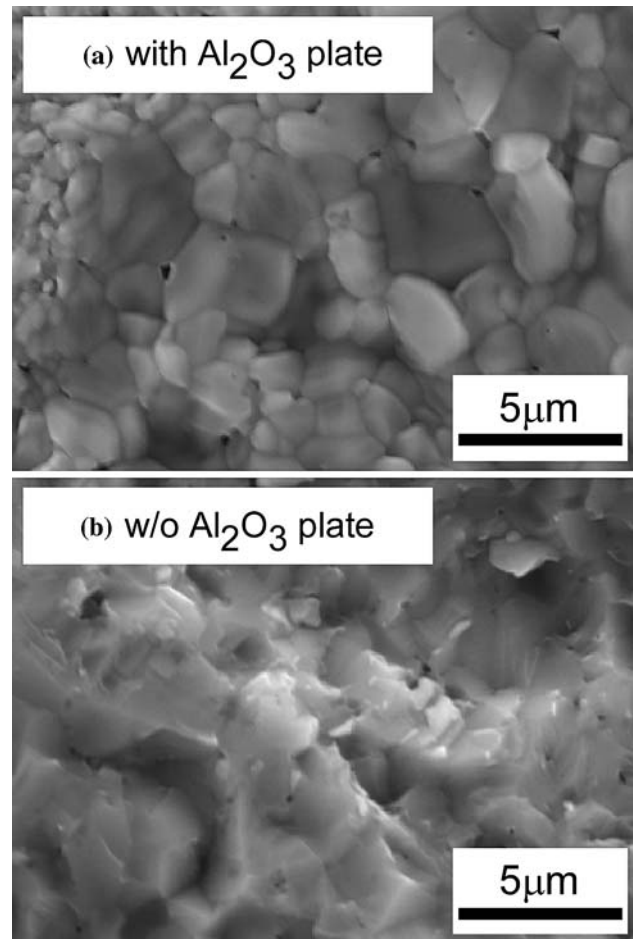


Fig. 8 Typical SEM cross section of sintered ZnO specimen. (a) With Al₂O₃ plate to control the internal current. (b) Without Al₂O₃ plate

condition is slightly same. On the other hand, the grain growth is different between current limited condition and conventional condition, and it suggests that internal current strongly influence of structure formation of ZnO specimen, especially the control of the grain growth.

Magnetic measurement of the internal current flow in the sintering specimen

In order to check the method for measurement of the internal current using a magnetic probe, calibration of the magnetic probe was conducted using an empty cylindrical graphite die. Figure 9 shows schematics of the graphite die and the position of magnetic probe in the die; Fig. 9a shows a vertical cross section of the empty graphite die, and Fig. 9b shows a horizontal cross section and position of the four turn coil in the magnetic probe with a radial direction from the central axis of the cylindrical die. In this experiment, it was assumed that the sintering current flows uniformly along the direction of the central axis of the

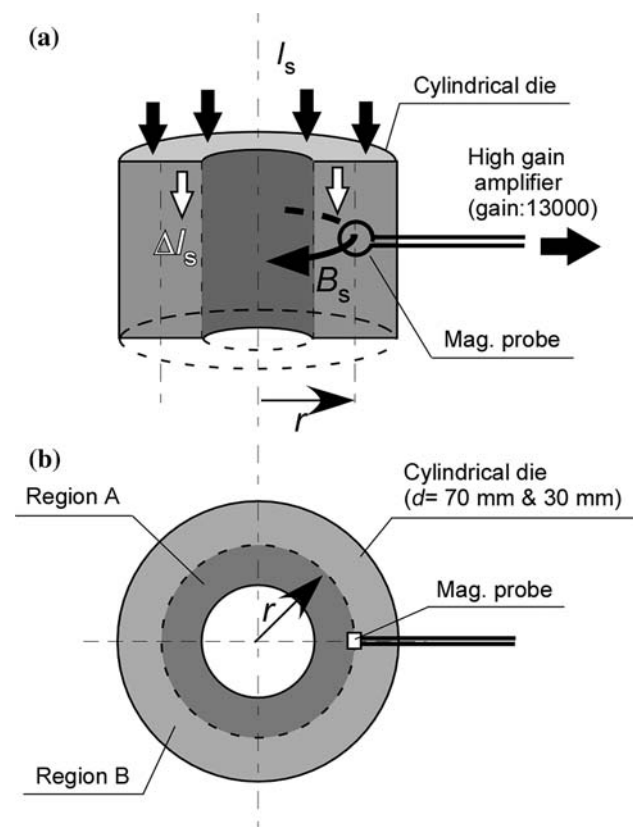


Fig. 9 Calibration setup of magnetic probe using empty cylindrical die. (a) Vertical cross section and relative position of magnetic probe and (b) horizontal cross section

cylindrical die. It is possible to change the position of the coil in the radial direction from $r = 0–25$ mm.

According to Ampere’s law (Eq. 2) and assuming axisymmetric current distribution, the magnetic probe can detect the magnetic field generated by a part of the sintering current only flowing in region A within the probe position r , as shown in Fig. 9b, and the current of the outer region B does not affect the magnetic field in the probe position. As a result, it is possible to estimate the distribution of internal current flow through the cylindrical die by changing the position of the magnetic probe. For example, when the inner and outer radii of the empty cylindrical die are a and b , respectively, and the total current I_s flows uniformly in the die, then the internal current ΔI_s the within probe position r ($a < r < b$) is evaluated using the following equation, and the magnetic field is generated in the same position,

$$\Delta I_s = I_s \cdot \frac{(r^2 - a^2)}{(b^2 - a^2)}. \tag{5}$$

Consequently, it is expected that the magnetic probe detects the magnetic field that depends on ΔI_s and r as shown in Eq. 3.

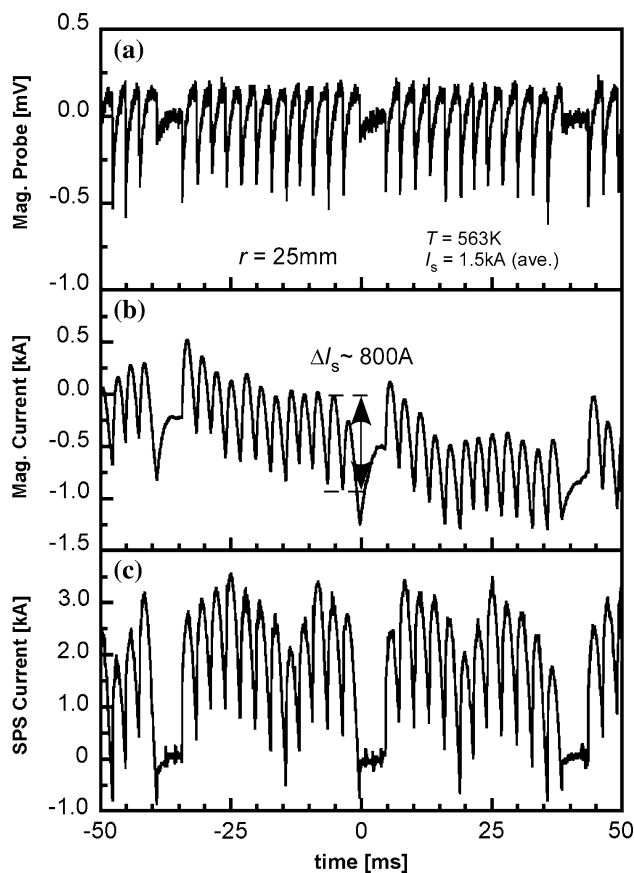


Fig. 10 Typical result of internal current estimated by magnetic probe. (a) Raw data of magnetic probe, (b) estimated internal current, and (c) total sintering current

Figure 10 shows a typical result of the internal current during the SPS process, measured using the magnetic probe located in the cylindrical die at $r = 25$ mm under sintering conditions of; gas pressure $P_{\text{gas}} = 5$ Pa, compressive pressure $P_{\text{press}} = 2.5$ MPa (almost non-compressive), heating rate $v_{\text{heat}} = 1$ K/s and maximum temperature $T_{\text{max}} = 773$ K (500 °C). Figure 10a shows the raw data for the counter electromotive force obtained using the magnetic probe, and Fig. 10b shows the internal current within $r = 25$ mm, which was evaluated by numerical time integration of the raw magnetic probe data, and Fig. 10c shows the raw sintering current data obtained from the SPS device. In the experiment, the current pattern of the SPS process is composed of a half wave pulse of 360 Hz; the turn-on period of the half wave pulse is 33 ms (12 pulses) and turn-off period is 5.6 ms (2 pulses), as shown in Fig. 10c.

It was found that the counter electromotive force detected by the magnetic probe has good temporal correlation with the waveform of the sintering current, and the waveform of Fig. 10a indicates the form of the time derivative of the sintering current from Fig. 10c. Therefore, it is considered that the magnetic probe can accurately

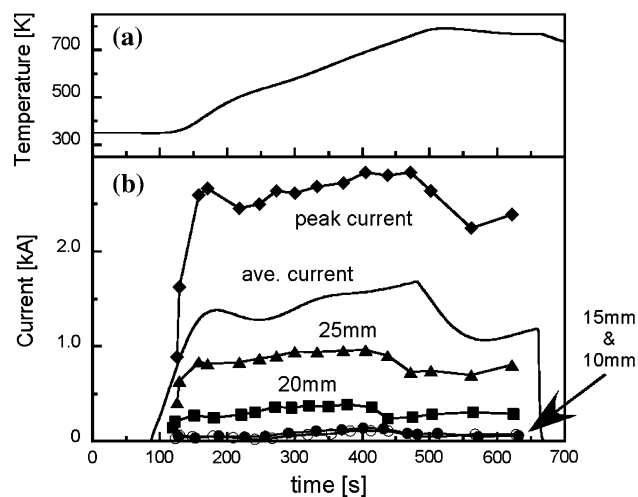


Fig. 11 Time evolution of internal current in the empty cylindrical die. (a) Temperature of empty die and (b) dependence of probe position

measure the internal current flow through the cylindrical die. The signal of the magnetic probe contains noise derived from the offset voltage of the amplifier or slowly fluctuated voltage by the thermoelectromotive force, etc., so that internal current is estimated by numerical integration of Fig. 10a, including the unnecessary low frequency components. Therefore, the useful signal for measurement of the internal current is the height of the half wave pulse, and the internal current was estimated to be approximately 800 A in Fig. 10b. The theoretical current calculated from Eq. 5 is approximately 900–1200 A, when $r = 25$ mm, $a = 15$ mm, $b = 35$ mm, and $I_s = 2.7$ –3.0 kA, so that the internal current measured using the magnetic probe almost agrees with the theoretical value.

Figure 11 shows the time evolution of the detected internal current when the position of the magnetic probe r is changed. The peak current in Fig. 11b is the peak value of the total sintering current, and ave. current is the averaged value of the total sintering current. The time evolution of the internal current has good correlation with the peak value of the sintering current for a probe position over $r = 15$ mm, and the internal current increase with the increase of probe position, as shown in Fig. 11.

The dependence of the detected internal current on the probe position is shown in Fig. 12. The current with $r = 35$ mm seems to be equal to the peak value of the total sintering current, and the solid and broken lines are theoretically evaluated from Eq. 5 at 473 and 773 K, respectively. According to Ampere's law (Eq. 2), a magnetic field cannot be formed inside the central bore, due to the absence of an internal current for $r = 15$ mm or less. It is anticipated that the internal current detected by the magnetic probe will increase in proportion to the square of the radial position r , according to Eq. 5.

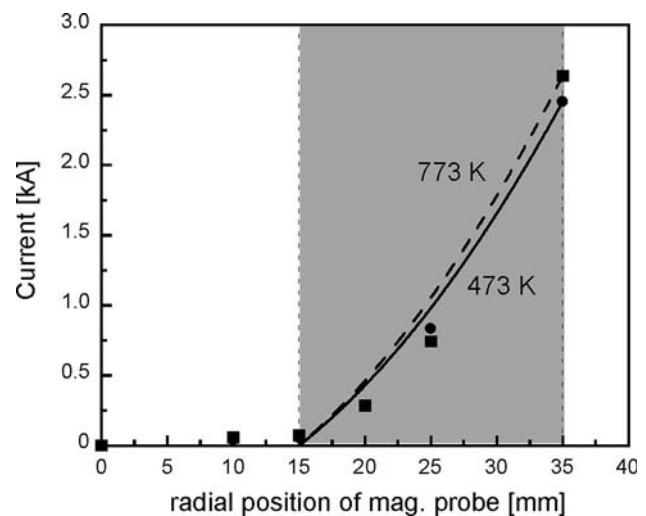


Fig. 12 Spatial distribution of internal current in the empty cylindrical die. Solid and broken lines are theoretical value estimated by Ampere's law

For positions of $r = 10$ and 15 mm, the internal current detected by the magnetic probe is sufficiently smaller than the peak of the sintering current. This proves that the coil of a magnetic probe inserted into a high temperature sintering die can accurately detect the magnetic field induced by the internal current only within probe position of r or less, and the influence of magnetic and thermal noise is negligibly small. In addition, it was clarified that the internal current measured by the magnetic probe changes in proportion to the square of the probe position, and quantitatively agrees with the theoretical value in the region of $r = 15$ –35 mm. The internal current flow through the sintering die and specimen can be quantitatively estimated by using the magnetic probe in the optional positions of the sintering die.

The time evolution of the internal current for the sintering of Cu powder was evaluated by magnetic probe, as shown in Fig. 13. The sintering conditions were as follows; quantity of Cu powder 40 g, gas pressure in the device $P_{\text{gas}} = 5$ Pa, compressive pressure $P_{\text{press}} = 2.5$ MPa, heating rate $v_{\text{heat}} = 1$ K/s, maximum temperature $T_{\text{max}} = 773$ K; the sintering die was maintained at the maximum temperature for 3 min. The magnetic probe was located on the side surface of the Cu powder; $r = 17.5$ mm.

Figure 13b shows the peak value of the sintering current (broken line and closed squares), the averaged sintering current (solid line) and the internal current evaluated using the magnetic probe (dotted line and closed circles). The peak value of the sintering current is the net current that flows inside the carbon graphite die and specimen, and the averaged sintering current is the averaged value of the peak current that was integrated using a passive integrating circuit composed of a resistor and capacitor. The averaged

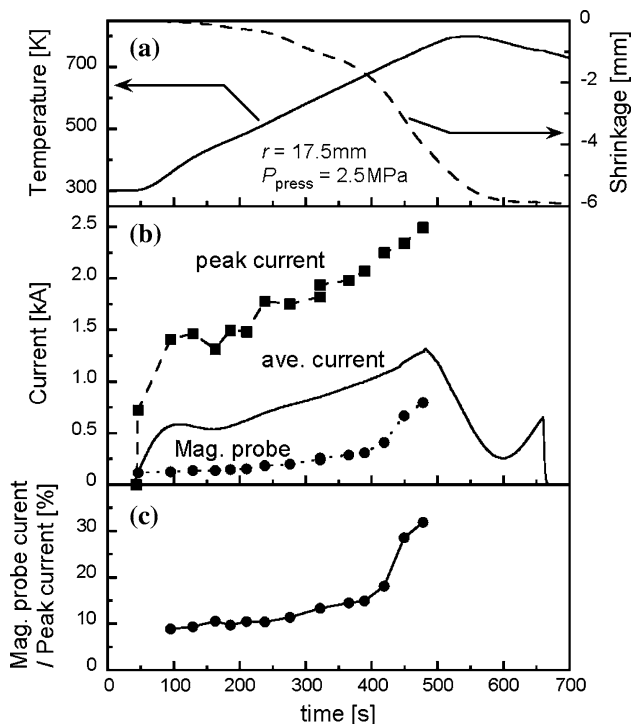


Fig. 13 Time evolution of internal current for the sintering of Cu powder. (a) Temperature of sintering die, (b) internal current, peak value, and average value of sintering current, and (c) ratio of internal current and peak value

sintering current becomes half of the peak value of the sintering current.

At the initial stage of the SPS process, the internal current measured using the magnetic probe is approximately 150 A, and the internal current gently increases with the increase in the peak value of the sintering current during $T = 300\text{--}600\text{ K}$. On the other hand, the internal current estimated using the magnetic probe drastically increases from 300 to 800 A over $T = 600\text{ K}$, and the shrinkage of the Cu specimen also significantly changes with the increase of the internal current in the same temperature region. In addition, the ratio of the internal current and the peak value of the total sintering current increases, as well as the temporal change of the internal current within $T = 300\text{--}600\text{ K}$, as shown in Fig. 13c. Over 30% of the sintering current can flow through the inside of the Cu specimen at the end stage of the SPS process. As a result, it is suggested that the temporal behavior of the internal current in the sintering specimen is related with the progress of sintering. It is also considered that the breakdown and destruction of the oxide insulating layer and the junction between Cu particles starts to cause an inflection point in the time evolution of the internal current.

The time evolution of the internal current for the sintering of ZnO powder with small additions of Al_2O_3 , TiO_2 , and CoO is shown in Fig. 14. The composition and

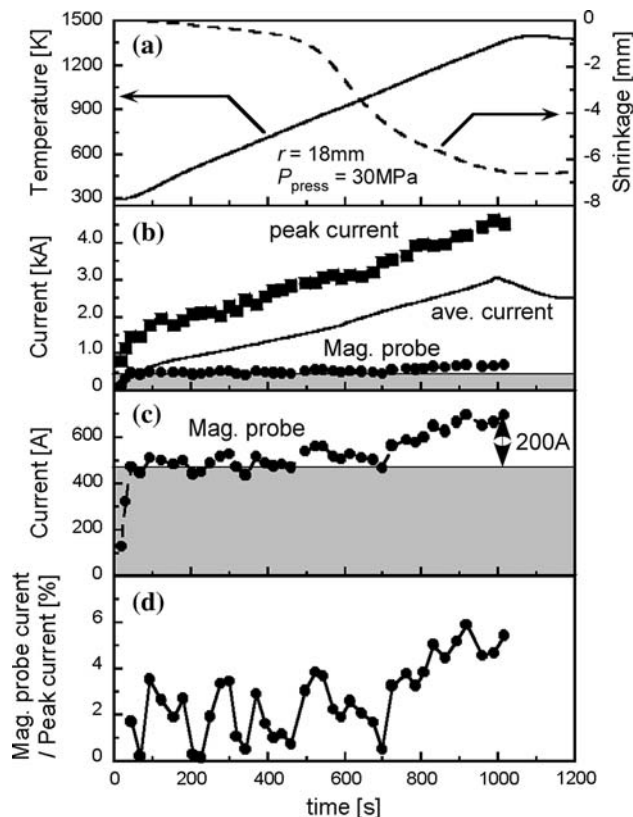


Fig. 14 Time evolution of internal current for the sintering of ZnO powder with small addition of Al_2O_3 , TiO_2 , and CoO . (a) Temperature of sintering die, (b) internal current, peak value, and average value of sintering current, (c) extended graph of internal current, and (d) ratio of internal current and peak value

preparation of ZnO powder is the same as that used for the previous experiment (Figs. 4 and 5). The sintering conditions used were as follows; quantity of ZnO powder 30 g, gas pressure in the device $P_{\text{gas}} = 5\text{ Pa}$, compressive pressure $P_{\text{press}} = 30\text{ MPa}$, heating rate $v_{\text{heat}} = 1\text{ K/s}$, maximum temperature $T_{\text{max}} = 1373\text{ K}$, and the sintering die was maintained at maximum temperature for 10 min. The magnetic probe was located on the side surface of the ZnO powder; $r = 18\text{ mm}$.

The internal current in the sintering ZnO powder changes with the increase of the sintering current and the temperature, as well as that for the sintering of the Cu powders, is shown in Fig. 13b. The internal current was approximately 500 A from the beginning of the SPS process and changed up to $T = 1100\text{ K}$, although the rate of increase was very small. However, when considering the results of Figs. 4 and 5, the electrical conductivity of ZnO powder is very large at the initial stage, and it is difficult for the internal current of several hundred amperes to flow in the raw ZnO powder.

The reason for the detection of unaccountable current is not clear, but it seems to be due to the imprecision of the

position of the magnetic probe in the sintering die. Theoretically, the coil of the magnetic probe should be sufficiently small, and the center position of the coil in the magnetic probe must be consistent with the radius of sintering specimen, $r = 15$ mm. However, it is not possible that the magnetic probe is located in the inside of sintering specimen because of crush by compressing force. As a result, the position of the coil of the magnetic probe become slightly outside from radius of sintering specimen (e.g., $r = 18$ mm in the case of Fig. 14), and the magnetic probe is able to detect the current that flows through the graphite region between the non-conductive powder and the center of the coil of magnetic probe (e.g., region of $r = 15$ – 18 mm in the case of Fig. 14). In this case, the unaccountable current was evaluated to be 500 A and this should be excluded.

The net value of the internal current flow through the ZnO powder increased with the increase of the sintering current from $T = 900$ K, and the maximum value was measured as approximately 200 A, as shown in Fig. 14c. Figure 14d shows the ratio of the internal current and the peak value of the sintering current, and the internal current in the specimen occupies approximately 6% of the total sintering current. The temperature of 900 K, from which the internal current starts to change, is in agreement with the temperature for the start of shrinkage, and this shows that the internal current increases with the progress of sintering.

Summary

In order to clarify the role of the internal pulsed current that flows in a sintering specimen in the SPS process, electric measurement of the resistance using Pt electrodes inserted in the specimen, and magnetic measurement of the internal pulsed current using a magnetic probe were carried out.

It was found that the resistance of the ZnO specimen with small additions of Al_2O_3 , TiO_2 , and CoO was significantly decreased under a very low temperature, compared with maximum temperature of sintering; the internal current may affect the sintering behavior and progress of the SPS process under a low temperature of 500 K. Sintering with internal current restriction using Al_2O_3 plates was carried out to observe the effect of internal current on sintering by the SPS process. The temperature dependence of the electrical resistance on the internal current limited condition is almost the same as that under conventional conditions; however, remarkable differences in the internal structure of the sintered specimens were observed. It was found that internal current that flows through the sintering material affects the formation of the internal structure during the SPS process.

To clearly observe the quantitative value and effect of the internal current on the SPS process, a magnetic measurement system using a magnetic probe was developed and applied to the internal current measurement of Cu and ZnO sintering by the SPS process. The accuracy of the measurement system was confirmed by the calibration experiment using an empty graphite die.

For the Cu powder sintering, the internal pulsed current in the Cu specimen drastically increased from 300 to 800 A as the sintering advanced. Breakdown and destruction of the oxide insulated layer and the junction between Cu particles caused an inflection point of time evolution of the internal current over $T = 600$ K. Thirty percentage of the sintering current can flow through the Cu specimen at the last stage of the SPS process. It was also found that internal current in the sintering specimen is related to the progress of sintering.

For the sintering of ZnO powder with small additions of Al_2O_3 , TiO_2 , and CoO , the internal current in the sintering ZnO powder changed with the increase of the sintering current, as for the sintering of Cu powder, although the quantitative value of the estimated current was comparatively small. The magnetic probe detected an unaccountable current caused by the inaccuracy of the position of the magnetic probe from the beginning of the SPS process. The net value of the internal current excluded the unaccountable value increase with the increase of sintering current over $T = 900$ K, and reached approximately 6% of the peak value of the total sintering current. The internal current started to change from a temperature of 900 K, which is in agreement with the temperature for the beginning of shrinkage, and it was confirmed that the internal current increases with the progress of sintering.

The measurement and estimation of an internal pulsed current using a magnetic probe in the specimen is very useful for in situ observation of the sintering behavior during the SPS process. However, limitations and problems do exist, and should be solved for more quantitative estimation of the internal pulsed current. It is anticipated that more accurate observation will be possible by the improvement of a highly accurate amplifier and integrator, calibration considering the temperature dependency of the electrical conductivity of the specimen and the sintering die, and compound measurements using multiple electrical and magnetic probes.

Acknowledgements The authors would like to thank Dr. K. Ozaki, Materials Research Institute for Sustainable Development, National Institute of Advanced Industrial Science and Technology (AIST), and Dr. Y. Makino, Joining and Welding Research Institute, Osaka University, for helpful discussion. The thorough and helpful comments of reviewers on this article are gratefully acknowledged. This research was partially supported by a Grant-in-Aid for Scientific Research (19740345, 2007) from the Ministry of Education, Science, Sports, and Culture of Japan.

References

1. Matsugi K, Hatayama T, Yanagisawa O (1995) *J Jpn Inst Met* 59:740
2. Omori M (2000) *Mater Sci Eng A* 287:183. doi:[10.1016/S0921-5093\(00\)00773-5](https://doi.org/10.1016/S0921-5093(00)00773-5)
3. Hwan-tae K, Kawahara M, Tokita M (2000) *J Jpn Soc Powder Powder Metall* 47:887
4. Yucheng W, Zhengyi F (2002) *Mater Sci Eng B* 90:34. doi:[10.1016/S0921-5107\(01\)00780-2](https://doi.org/10.1016/S0921-5107(01)00780-2)
5. Chen W, Anselmi-Tamburini U, Garay JE, Groza JR, Munir ZA (2005) *Mater Sci Eng A* 394:132. doi:[10.1016/j.msea.2004.11.020](https://doi.org/10.1016/j.msea.2004.11.020)
6. Anselmi-Tamburini U, Gennari S, Garay JE, Munir ZA (2005) *Mater Sci Eng A* 394:139. doi:[10.1016/j.msea.2004.11.019](https://doi.org/10.1016/j.msea.2004.11.019)
7. Anselmi-Tamburini U, Garay JE, Munir ZA (2005) *Mater Sci Eng A* 407:24. doi:[10.1016/j.msea.2005.06.066](https://doi.org/10.1016/j.msea.2005.06.066)
8. Munir ZA, Anselmi-Tamburini U, Ohyanagi M (2006) *J Mater Sci* 41:763. doi:[10.1007/s10853-006-6555-2](https://doi.org/10.1007/s10853-006-6555-2)
9. Jackson JD (1975) *Classical electrodynamics*. Wiley & Sons, Inc, 174 p